Potent VEGF blockade causes regression of coopted vessels in a model of neuroblastoma

Eugene S. Kim*, Anna Serur*, Jianzhong Huang*, Christina A. Manley†, Kimberly W. McCrudden*, Jason S. Frischer*, Samuel Z. Soffer*, Laurence Ring†, Tamara New†, Stephanie Zabski‡, John S. Rudge‡, Jocelyn Holash‡, George D. Yancopoulos‡, Jessica J. Kandel*, and Darrell J. Yamashiro*†§

Divisions of *Pediatric Surgery and †Pediatric Oncology, College of Physicians and Surgeons of Columbia University, New York, NY 10032; and ‡Regeneron Pharmaceuticals, Incorporated, 777 Old Saw Mill River Road, Tarrytown, NY 10591

Communicated by P. Roy Vagelos, Merck & Co., Inc., Bedminster, NJ, July 5, 2002 (received for review April 19, 2002)

Vascular endothelial growth factor (VEGF) plays a key role in human tumor angiogenesis. We compared the effects of inhibitors of VEGF with different specificities in a xenograft model of neuroblastoma. Cultured human neuroblastoma NGP-GFP cells were implanted intrarenally in nude mice. Three anti-VEGF agents were tested: an anti-human $VEGF_{165}$ RNA-based fluoropyrimidine aptamer; a monoclonal anti-human VEGF antibody; and VEGF-Trap, a composite decoy receptor based on VEGFR-1 and VEGFR-2 fused to an Fc segment of IgG1. A wide range of efficacy was observed, with high-dose VEGF-Trap causing the greatest inhibition of tumor growth (81% compared with controls). We examined tumor angiogenesis and found that early in tumor formation, cooption of host vasculature occurs. We postulate that this coopted vasculature serves as a source of blood supply during the initial phase of tumor growth. Subsequently, control tumors undergo vigorous growth and remodeling of vascular networks, which results in disappearance of the coopted vessels. However, if VEGF function is blocked, cooption of host vessels may persist. Persistent cooption, therefore, may represent a novel mechanism by which neuroblastoma can partly evade antiangiogenic therapy and may explain why experimental neuroblastoma is less susceptible to VEGF blockade than a parallel model of Wilms tumor. However, more effective VEGF blockade, as achieved by high doses of VEGF-Trap, can lead to regression of coopted vascular structures. These results demonstrate that cooption of host vasculature is an early event in tumor formation, and that persistence of this effect is related to the degree of blockade of VEGF activity.

It is well established that the growth and metastasis of solid tumors depend on angiogenesis. Many studies have shown that one mechanism by which tumors induce the formation of new blood vessels is expression of proangiogenic factors. The most commonly implicated factor is vascular endothelial growth factor (VEGF), a specific endothelial cell mitogen, permeability, and survival factor, overexpressed in virtually all human tumors (1). Antagonism of the VEGF pathway results in inhibition of angiogenesis and tumor growth in a number of tumor model systems (2).

In previous studies, we have shown that the degree of efficacy of VEGF suppression differs markedly in different experimental tumors. Despite similar levels of initial VEGF expression, after administration of anti-VEGF antibody, both primary tumor growth and metastasis were nearly completely eradicated in experimental Wilms tumors, whereas in a parallel model of neuroblastoma, tumor growth was only moderately affected with persistence of metastasis (3, 4). This difference in response to antiangiogenic therapy suggests that other mechanisms may support perfusion and tumor growth in neuroblastoma.

Recruitment or cooption of preexisting blood vessels by tumors, as previously described by Holash and colleagues, may represent one such mechanism (5–7). Early in tumor development, preexisting vasculature is engaged by growing tumor cells. Subsequently, the coopted vessels regress. The tumor becomes hypoxic, VEGF expression is up-regulated, and neoangiogenesis is induced. In other studies, vascular cooption in experimental glioblastoma after tumors were exposed to VEGF blockade suggests that this mechanism may also be invoked by established tumors deprived of VEGF (8, 9).

We have recently examined vascular cooption in a xenograft model of neuroblastoma (10). Neuroblastoma tumor cells implanted into the kidney of nude mice result in large vascular tumors. Treatment with an anti-VEGF antibody causes partial tumor inhibition, decreased angiogenesis, and by angiography results in the appearance of novel rounded structures at vessel branches, which we had initially termed "terminal vascular bodies" (10). In the current study, we demonstrate that these structures are in fact renal glomeruli that have been coopted by tumor tissue. This cooption is an early event in tumor growth in experimental neuroblastoma, because it is present in both control xenografts and tumors treated with the anti-VEGF agents [monoclonal anti-VEGF antibody (11) and VEGF-Trap, a composite decoy receptor based on VEGF receptor-1 (VEGFR-1) and VEGFR-2 fused to an Fc segment of IgG1 (12)]. In control neuroblastomas, this stage is followed by vascular remodeling in conjunction with brisk angiogenesis; coopted glomeruli disappear. However, in tumors treated with either anti-VEGF antibody or low-dose VEGF-Trap, cooption persists, permitting perfusion and ongoing tumor growth. Treatment with high-dose VEGF-Trap results in stunted tumors, which are virtually avascular and in which only rare coopted glomeruli are present, suggesting that the coopted vasculature has regressed. These studies demonstrate that cooption of host vasculature occurs early in neuroblastoma tumor growth. Persistent cooption appears to depend on an intermediate degree of VEGF blockade and may result in the relative resistance of a specific tumor to antiangiogenic therapy, which may be overcome by a higher degree of VEGF blockade.

Methods

Cell Line. The human neuroblastoma cell line NGP, which had previously been transfected with a retroviral vector containing enhanced green fluorescent protein, was maintained in culture in 75-cm^2 flasks with McCoy's 5A medium (Mediatech, Fisher Scientific). Medium was supplemented with 10% FBS and 1% penicillin/streptomycin (GIBCO). Cells were grown at 37°C in 5% CO_2 until confluent. NGP-GFP cells were harvested by trypsinization, counted with trypan blue staining, and washed and resuspended in sterile saline solution (phosphate buffered saline, GIBCO) at a concentration of 10^7 cells/ml.

Animal Model. All experiments were approved by the Institutional Animal Care and Use Committee of Columbia University. Female NCR nude mice, 4–6 weeks of age (Taconic Farms),

Abbreviations: VEGF, vascular endothelial growth factor; rVEGF, VEGF receptor; LD, low dose; HD, high dose; αSMA, α-smooth muscle actin; TUNEL, terminal deoxyribonucleic d-UTP nick end labeling.

§To whom reprint requests should be addressed. E-mail: dy39@columbia.edu.

were housed in a barrier facility and acclimated to 12-hr light/dark cycles for at least 1 day before use.

Tumor Implantation. The left flank was prepared in a sterile manner after anesthetizing the mice with i.p. ketamine (50 mg/kg) and xylazine (5 mg/kg). An incision was made exposing the left kidney, and an inoculum of 10^6 NGP-GFP tumor cells in 0.1 ml of PBS was injected with a 25-g needle. The flank muscles were closed with a single 4–0 Polysorb suture (US Surgical, Norwalk, CT) and the skin closed with staples.

Antiangiogenic Treatment. There were three sets of experiments, each with its own set of control tumors: (*i*) NX1838, a RNA-based fluoropyrimidine polyethylene glycol-conjugated aptamer targeting human $VEGF_{165}$ (NeXstar, Boulder, CO) (13, 14) at 250 μg per dose NX1838 ($n = 5$) or vehicle control (0.05% mouse serum albumin, Sigma, $n = 5$) injected i.p. daily; (*ii*) humanized monoclonal anti-VEGF antibody (A4.6.1, Genentech) (11), at 100 μg/dose ($n = 19$) or vehicle control ($n = 21$) administered i.p. biweekly; and (*iii*) 100 μg per dose [low dose (LD), VEGF-Trap LD, $n = 10$], 500 μg per dose [high dose (HD), VEGF-Trap HD, $n = 10$] VEGF-Trap (Regeneron Pharmaceuticals, Tarrytown, NY) (12), or vehicle control ($n = 21$) administered i.p. biweekly. Treatment began 3 or 4 days after tumor implantation and continued for 5.5 weeks (6-week time point). An additional set of mice (four mice for control, anti-VEGF antibody, VEGF-Trap LD, and VEGF-Trap HD) were examined after 3.5 weeks of treatment (4-week time point).

Fluorescein Angiograms. Fluorescein angiography for demonstration of vascular architecture was performed as previously described (9). After anesthetizing the mice with i.p. ketamine (50 mg/kg) and xylazine (5 mg/kg), a sternotomy was performed to expose the heart. Five percent fluorescein isothiocyanate–dextran (2,000,000 M_r, Sigma) in a volume of 1-cc PBS was injected into the left ventricle. After perfusion of the tumor, mice were killed.

Harvesting of Specimens. After death of mice, tumors and contralateral kidneys were removed. One-half of each kidney/tumor was fixed in fresh 4% paraformaldehyde for histology and immunohistochemistry at room temperature. The other half was flash frozen in liquid nitrogen and stored at −80°C. Paraformaldehyde-fixed specimens were subsequently embedded in paraffin blocks.

Immunohistochemistry. *α-Smooth muscle actin (αSMA) staining.* A monoclonal anti-αSMA actin antibody (Sigma) was diluted (1:200), and incubated overnight at 4°C. Specimens were then incubated in turn with a 1:400 rabbit anti-mouse biotinylated secondary antibody (Zymed). Enhanced horseradish peroxidase-conjugated streptavidin and a substrate chromogen, AEC (3-amino-9-ethyl carbazole), was used to develop a brown–red color (HistoStain-Plus kit, Zymed).

Terminal deoxyribonucleic d-UTP nick end labeling (TUNEL) assay. Mounted paraformaldehyde-fixed specimens underwent TUNEL assay for apoptosis by using the In Situ Cell Death Kit (Roche Applied Science, Indianapolis) and were examined by light microscopy.

***In Situ* Hybridization.** Tissue was initially preserved in 4% paraformaldehyde overnight, transferred to 17% sucrose, and embedded in OCT compound and frozen. Tissue sections were then probed with ^{35}S-labeled cRNA with a probe spanning codons 57–192 of human VEGF as described (6).

Statistical Analysis. Tumor weights were expressed as mean ± SEM and compared by Kruskal–Wallis analysis.

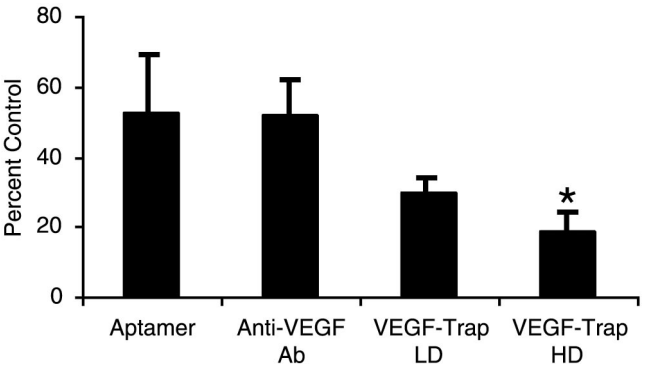

Fig. 1. Inhibition of neuroblastoma tumors by anti-VEGF agents. Neuroblastoma xenografts were treated with the anti-VEGF agents (NX1838, $n = 5$; anti-VEGF antibody, $n = 19$; VEGF-Trap LD, $n = 10$; and VEGF-Trap HD, $n = 10$), with the results expressed as percent of control tumors (control NX1838, $n = 5$; control anti-VEGF antibody, $n = 21$; control VEGF-Trap LD, $n = 10$; and control VEGF-Trap HD, $n = 10$), with error bars representing SEM for treated tumors. Statistical analysis was done by Kruskal–Wallis analysis, with NX1838 ($P = 0.08$), anti-VEGF antibody ($P = 0.12$), VEGF-Trap LD ($P = 0.10$), and VEGF-Trap HD ($P = 0.0009$).

Results

Comparison of Anti-VEGF Reagents in Experimental Neuroblastoma. Using a metastasizing murine model of neuroblastoma (3), we tested the effects of anti-VEGF reagents with differing targets. We evaluated NX1838, an RNA-based fluoropyrimidine polyethylene glycol-conjugated aptamer, which has an estimated dissociation constant (K_d) for human $VEGF_{165}$ of 200 pM (NeXstar) (13, 14); the monoclonal anti-VEGF antibody (A.4.6.1, Genentech) (11) that specifically binds to human VEGF with an affinity of 0.1–10 nM but not murine VEGF; and VEGF-Trap, a soluble composite decoy receptor consisting of Ig-like domains of VEGFR-1 and VEGFR-2 fused to an Fc segment (VEGF-Trap, Regeneron Pharmaceuticals) (12), which binds with very high affinity (≈1 pM) to multiple isoforms of VEGF from several species (including human and murine). The VEGF-Trap also binds to placental growth factor. Tumor weight was evaluated at 6 weeks.

We found that treatment with NX1838 and anti-VEGF antibody resulted in partial inhibition of tumor growth (Fig. 1, 52 and 53% of control, respectively, $P = 0.08$ and $P = 0.12$, respectively). We also tested the efficacy of VEGF-Trap at two doses, 100 μg (VEGF-Trap LD) and 500 μg (VEGF-Trap HD). VEGF-Trap LD partially suppressed tumor growth (30% of control, $P = 0.10$), whereas VEGF-Trap HD displayed the highest degree of tumor suppression of the antiangiogenic agents tested (19% of control, $P = 0.009$) (Fig. 1). These results demonstrate that VEGF-Trap at 500 μg per dose can significantly suppress tumor growth in our xenograft model of neuroblastoma.

Vascular Cooption Is an Early Event in Neuroblastoma Tumor Growth. We next performed a detailed comparison of angiogenesis in the control tumors with the anti-VEGF antibody and VEGF-Trap-exposed tumors (because of the limited supply of NX1838, we were unable to conduct a more detailed analysis). We examined angiogenesis by fluorescein angiography and αSMA immunostaining at 4 and 6 weeks. At 4 weeks, fluorescein perfusion outlined rounded structures at the branch points of vessels in control, anti-VEGF antibody-treated, VEGF-Trap LD, and VEGF-Trap HD tumors (Fig. 2 *A–D*, respectively; see white arrowheads). Closer examination by confocal microscopy suggested that the structures (about 80 microns in diameter) were renal glomeruli, with afferent and efferent blood vessels (Fig. 2 *E–H*, respectively). Entrapment of renal glomeruli within tumor

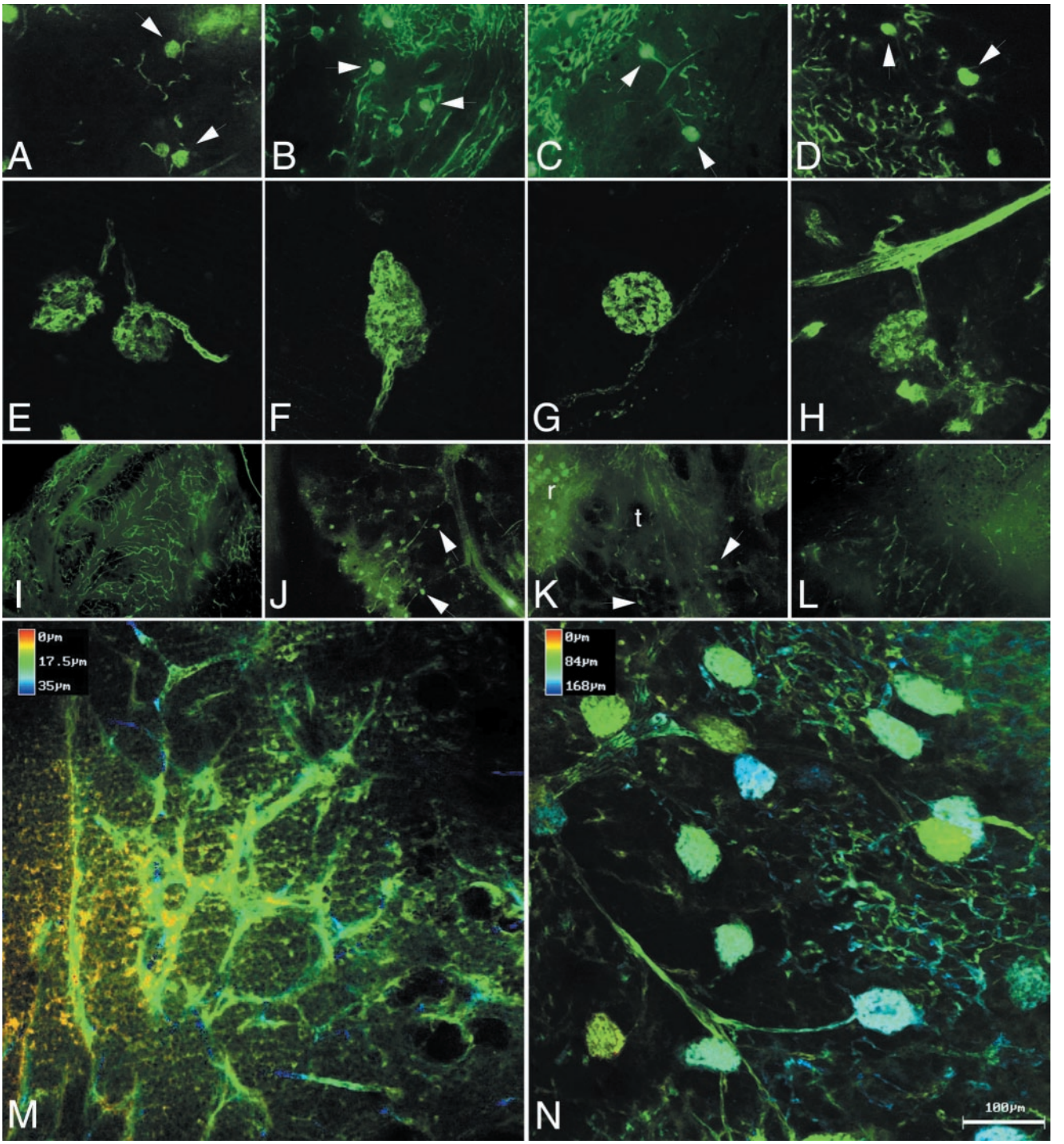

Fig. 2. Fluorescein angiography. Tumor vasculature was evaluated by fluorescein–dextran angiography at 4 (*A–H*) and 6 weeks (*I–N*). At 4 weeks, standard fluorescent microscopy (*A–D*, ×10 original magnification) revealed cooption of renal glomeruli in Control (*A*), anti-VEGF antibody (*B*), VEGF-Trap LD (*C*), and VEGF-Trap HD (*D*). Close-up view of coopted glomeruli by confocal microscopy: Control (*E*), anti-VEGF antibody (*F*), VEGF-Trap LD (*G*), and VEGF-Trap HD (*H*), demonstrates connection of glomeruli to afferent and efferent vessels, seen in best in *E* and *G*. At 6 weeks, standard fluorescent microscopy (*I–L*, ×4 original magnification) demonstrates vascular remodeling with abundant vessels in control tumors (*I*), but persistent cooption in the anti-VEGF antibody (*J*) and VEGF-Trap LD (*K*), with glomeruli indicated by arrowheads. In VEGF-Trap HD (*L*), sparse vasculature and little cooption were seen at 6 weeks. Pseudodepth coloring of Control (*M*) and anti-VEGF antibody (*N*), demonstrates the abundant vasculature in Control tumors, and the persistent cooption in the anti-VEGF antibody-treated tumors. The coopted glomeruli are approximately 80 μm in size (Bar = 100 μm.).

tissue was evident after hematoxylin/eosin staining in control (Fig. 3 *A* and *E*), anti-VEGF antibody (Fig. 3 *B* and *F*), VEGF-Trap LD (Fig. 3 *C* and *G*), and VEGF-Trap HD (Fig. 3 *D* and *H*). At the interface of tumor–kidney invasion, the tumor cells replace the renal parenchyma; however, glomeruli are preserved, becoming encased in tumor. Red blood cells are visible within the glomeruli, indicating that these structures remain perfused, despite being surrounded by tumor tissue.

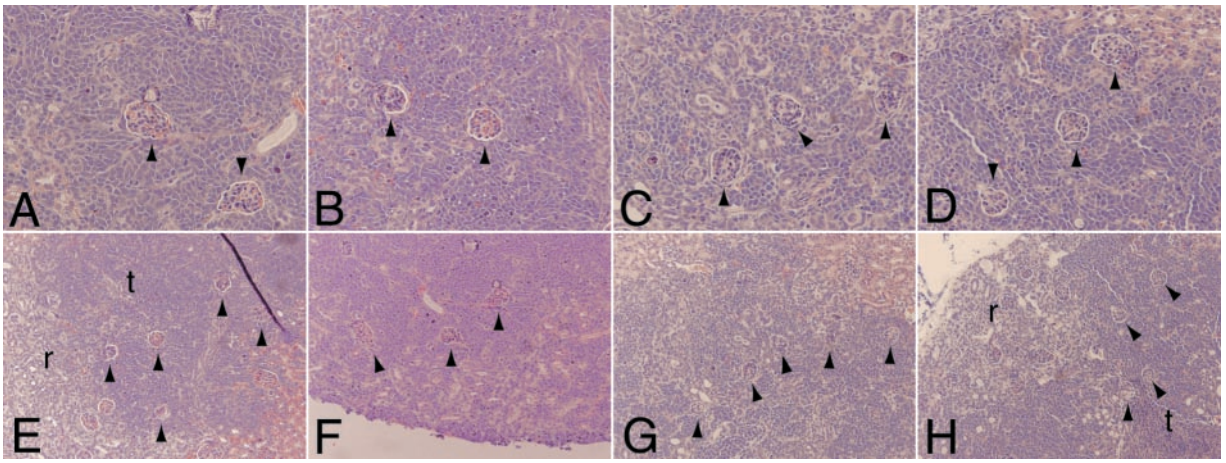

Fig. 3. Cooption of renal glomeruli at 4 weeks. Early in tumor growth, all tumors demonstrate cooption of renal glomeruli (arrowheads) as seen by hematoxylin/eosin staining (*A–D*, ×20; *E–F*, ×10): Control (*A* and *E*), anti-VEGF antibody (*B* and *F*), VEGF-Trap LD (*C* and *G*), and VEGF-Trap HD (*D* and *H*). In control (*E*) and VEGF-Trap HD (*H*), coopted glomeruli (arrowheads) encased by tumor tissue (t) are seen adjacent to renal tissue (r).

These results demonstrate that cooption of renal vasculature and glomeruli occurs early in tumor growth.

At 6 weeks, control tumor growth was characterized by vascular remodeling with abundant new vessels (Fig. 2 *I* and *M*). We did not detect glomerular cooption in 6-week controls either by fluorescein angiography or by hematoxylin/eosin staining (data not shown). In contrast, 6-week xenografts exposed to anti-VEGF antibody or VEGF-Trap LD displayed persistent vascular cooption both by fluorescein angiography (anti-VEGF antibody, Fig. 2 *J* and *N*; VEGF-Trap LD, Fig. 2*K*) and hematoxylin/eosin staining (data not shown). Confocal microscopy demonstrates that the multiple coopted glomeruli are perfused by branches originating from long straight vessels (anti-VEGF antibody, Fig. 2*N*). When anti-VEGF antibody and VEGF-Trap LD therapy are stopped, these vascular structures are lost within 3 weeks and replaced by abundant new vessels, suggesting that neoangiogenesis had remodeled the originally coopted structure (data not shown). In the VEGF-Trap HD group, tumors at 6 weeks had very sparse vasculature with little glomeruli cooption seen by angiography (Fig. 2*L*). Because fluorescein–dextran angiography will demonstrate only perfused glomeruli, we also examined sections stained by hematoxylin/eosin to determine whether nonperfused glomeruli remained within the tumor tissue. By using this method of examination, again only rare glomeruli were seen (data not shown), indicating that there was near complete regression of the coopted vascular structure that was seen at 4 weeks. These results demonstrate that partial or incomplete blockade of VEGF can block vascular remodeling and elicit persistent vascular cooption in experimental neuroblastoma, whereas more complete VEGF blockade results in regression of the coopted vasculature and a more profound antitumor effect.

Anti-VEGF Reagents Result in Decreased Vasculature. Staining for αSMA immunopositive cells was performed to further evaluate recruitment of perivascular cells (15). Control tumors displayed a dense perivascular network at 4 (Fig. 4*A*) and 6 weeks (Fig. 4*E*). Animals injected with anti-VEGF antibody, VEGF-Trap LD, and VEGF-Trap HD developed tumors with markedly decreased αSMA-staining vascular components as compared with controls at both 4 (Fig. 4 *B–D*) and 6 weeks (Fig. 4 *F–H*). Similarly, markedly decreased endothelium was also seen by immunostaining for the endothelial marker platelet–endothelial cell adhesion molecules-1 (data not shown). When injections of

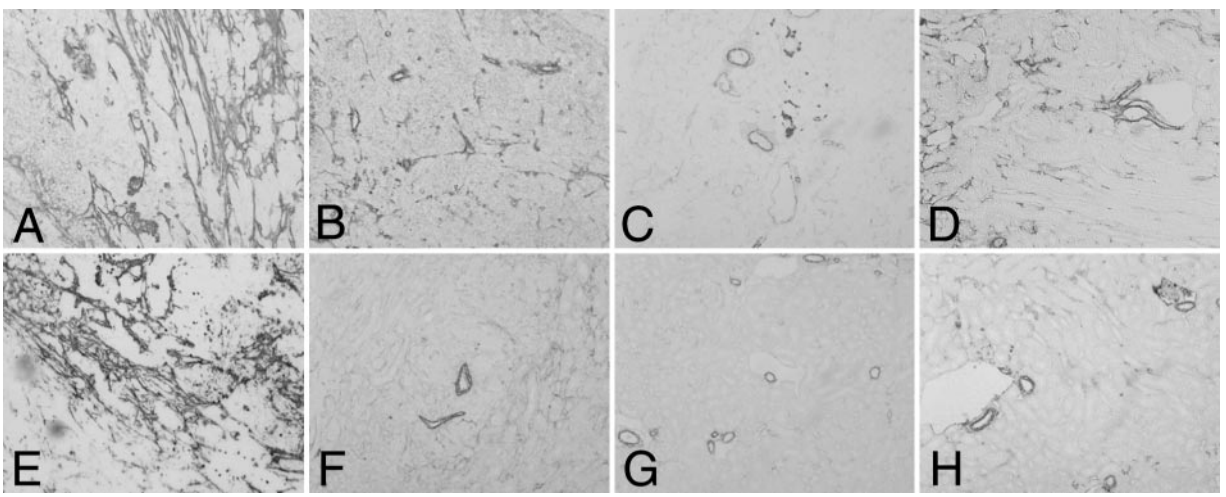

Fig. 4. Decreased vascularity (reflected by diminished recruitment of perivascular cells) is seen by αSMA staining. Four (*A–D*) and 6 weeks (*E–H*), ×10 original magnification. Control (*A* and *E*) tumors have abundant vasculature and are associated with numerous perivascular cells. There was marked decrease in neoangiogenesis with only a few larger-caliber vessels in tumors after injection of anti-VEGF antibody (*B* and *F*), VEGF-Trap LD (*C* and *G*), and VEGF-Trap HD (*D* and *H*).

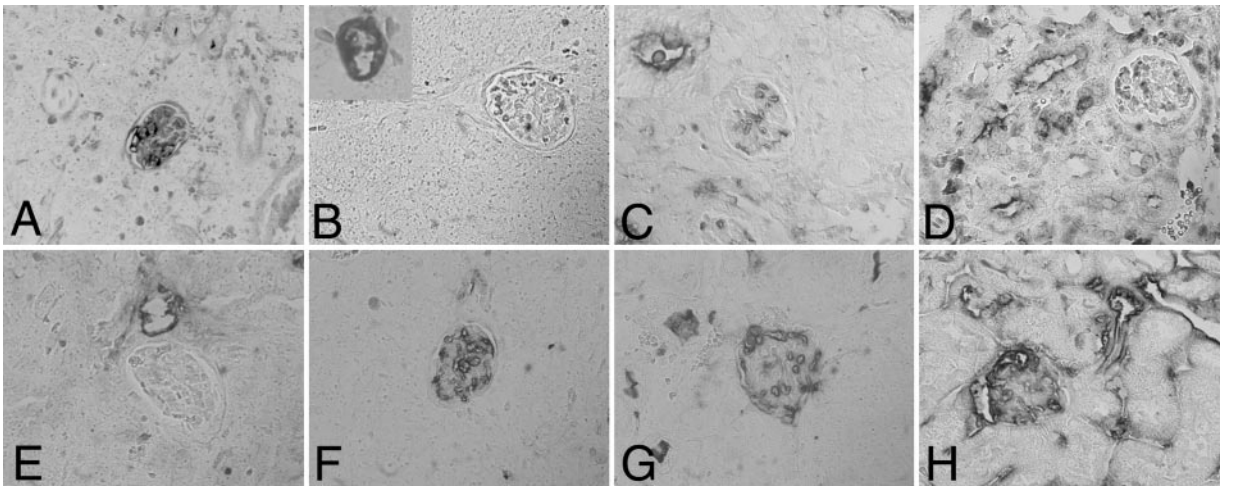

Fig. 5. Apoptosis in renal glomeruli. Apoptosis was evaluated at 4 (*A–D*) and 6 weeks (*E–H*) by TUNEL. Control (*A* and *E*), anti-VEGF antibody (*B* and *F*), VEGF-Trap LD (*C* and *G*), and VEGF-Trap HD (*D* and *H*). Endothelial apoptosis was seen in anti-VEGF antibody (*Inset B*), VEGF-Trap LD (*Inset C*), and VEGF-Trap HD (*D*) but rarely in control tumors (*A*). Both control tumors and VEGF-Trap HD demonstrated apoptosis within glomeruli, suggesting that in tumors where cooption is transient, glomeruli undergo early apoptosis. Red blood cells are seen in the glomeruli of anti-VEGF antibody (*B*) and VEGF-Trap LD (*C*) tumors, but there is little apoptosis within the glomeruli. Apoptosis within glomeruli is seen at a later time point (6 weeks) in the anti-VEGF antibody (*F*) and VEGF-Trap LD (*G*) tumors.

anti-VEGF agent were withheld for 2 weeks, 8-week tumors demonstrated increased blood vessel development compared with their 6-week counterparts (data not shown).

Anti-VEGF Reagents Result in Endothelial and Glomerular Apoptosis. To explore the mechanism of decreased angiogenesis seen with anti-VEGF treatment, TUNEL assays were performed to detect the presence of apoptosis, particularly in the endothelial cells and glomeruli. Control tumors had little apoptosis in endothelial cells at 4 or 6 weeks (Fig. 5 *A* and *E*). In the treated tumors (anti-VEGF antibody, VEGF-Trap LD, and VEGF-Trap HD) at 4 weeks, endothelial cell apoptosis was observed (Fig. 5 *B–D*). At 4 weeks, apoptosis was found in coopted glomeruli in the control and VEGF-Trap HD tumors but rarely in the VEGF-Trap LD or anti-VEGF antibody-exposed tumors. At 6 weeks, however, there was marked apoptosis within glomeruli in all three anti-VEGF-treated groups (Fig. 5 *F–H*). The presence of apoptosis within glomeruli at 4 weeks is consistent with the absence of these structures at 6 weeks in the control and VEGF-Trap HD groups and contrasts with the status of coopted glomeruli in VEGF-Trap LD and anti-VEGF antibody-treated tumors. Apoptosis in glomeruli outside of the tumor mass was not observed. Our results suggest that very efficient blockade of VEGF with VEGF-Trap HD overrides factors tending to preserve coopted glomeruli in VEGF-deprived neuroblastoma xenografts, resulting in endothelial apoptosis and involution of these coopted vascular structures.

Anti-VEGF Reagents Result in VEGF Up-Regulation. To evaluate VEGF expression in these tumors, *in situ* hybridization was performed by using a probe that crossreacts with both mouse and human VEGF. At 4 weeks, all xenografts demonstrated a diffuse low level of VEGF expression (data not shown). At 6 weeks, the control xenografts continued to demonstrate a diffuse low level of VEGF expression (Fig. 6*A*). Treatment of xenografts with the anti-VEGF reagents resulted in marked increase in VEGF expression in the anti-VEGF antibody, VEGF-Trap LD and VEGF-Trap HD tumors (Fig. 6 *B–D*, respectively). These results suggest that the blockade of VEGF and the resultant decrease in perfusion, via decreased neoangiogenesis and endothelial apoptosis, lead to tumor hypoxia and a strong up-regulation in VEGF expression. Hypoxia-induced VEGF expression in tumors may serve as a useful surrogate for the effectiveness of antiangiogenesis agents.

Discussion

Our data are consistent with a model in which certain tumors, such as neuroblastomas, initially coopt host vasculature and then remodel this host vasculature, destroying the initial coopted structures. These results further lead to the hypothesis that such cooption can be dramatically and differentially affected by the degree of VEGF blockade. Partial VEGF blockade, as may be achieved by the anti-VEGF antibody A4.6.1, or low-dose VEGF-Trap, allows for initial vessel cooption but inhibits later remodeling, resulting in long-term persistence of the coopted vascular

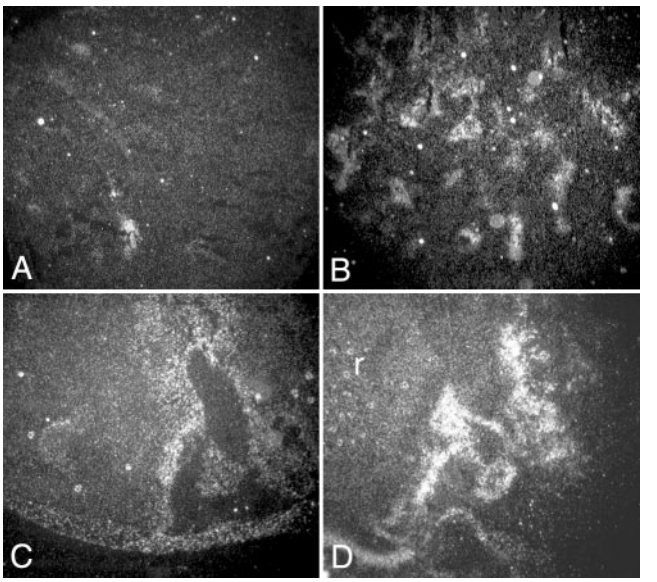

Fig. 6. Anti-VEGF treatment results in up-regulation of VEGF expression. *In situ* hybridization demonstrated a low-level diffuse expression of VEGF in control (*A*) tumors at 6 weeks, but marked up-regulation of VEGF in anti-VEGF antibody (*B*), VEGF-Trap LD (*C*), and VEGF-Trap HD (*D*) tumors at the same time point. In *D*, renal tissue is present (r) and contains glomeruli that express VEGF.

structures. The lack of vascular growth results in a poorly perfused tumor, which in turn results in hypoxic induction of VEGF in the tumor and thus reflects successful blockade of angiogenesis. More complete VEGF blockade, as effected in these studies by the high-dose VEGF-Trap, results in a modification of the above events. As with partial VEGF inhibition, initial vascular cooption occurs and subsequent remodeling is also blocked, leaving the coopted vasculature intact in the short term. In contrast to partial VEGF inhibition, however, it appears that more complete blockade eventually leads to regression of the coopted vasculature. In this setting, tumor growth is also significantly more inhibited, indicating that persistent coopted vessels can indeed support some tumor growth, even in the absence of new angiogenesis.

One possible explanation for this disparate effect of high-dose VEGF-Trap, as compared with anti-VEGF antibody or low-dose VEGF-Trap, is that at this dose this agent efficiently blocks not just the VEGF required for new vasculature to sprout but also the low levels of this factor required to support the long-term integrity of coopted vasculature. As a result, the coopted structures undergo apoptosis. Tumor growth is more effectively suppressed than if neoangiogenesis alone were inhibited.

The ability of high-dose VEGF-Trap to disrupt cooption may be a consequence of its higher affinity for human VEGF than that of the anti-VEGF antibody A4.6.1, or the prolonged circulation time of the VEGF-Trap (11, 12). Thus, VEGF-Trap may be able to more completely block the human VEGF derived from the implanted human tumors. Alternatively, because VEGF-Trap also binds mouse VEGF (12), which is not recognized by the anti-VEGF antibody A4.6.1 (13), its greater efficacy could be because of blockade of both tumor-derived (human) as well as host-derived (murine) VEGF. Finally, the increased efficacy of the high-dose VEGF-Trap compared with the VEGF antibody may be because of its ability to bind VEGF family members other then VEGF A, such as placental growth factor, which is known to bind this agent (14). However, we did not test either the NX1838 aptamer or anti-VEGF antibody at higher doses, so it is possible that increased concentrations of these anti-VEGF agents would cause a more complete blockade of tumor growth as well as disrupting cooption.

Determination of the relative contribution of low-level VEGF and other VEGF family members to cooption of host vessels will depend on the development of new probes to individually differentiate these factors. Our results suggest that the ability of neuroblastoma to support continued growth via cooption of preexisting vasculature represents an important mechanism of tumor resistance to antiangiogenic treatment and may require adjustment of these emerging therapies to counter such responses.

We are grateful to A. Lalla for technical assistance. This work was supported by the Pediatric Cancer Foundation (J.J.K. and D.J.Y.), the Sorkin Fund, (J.J.K.), and National Cancer Institute Grant 1R01CA088951-01A1 (D.J.Y.).

1. Leung, D. W., Cachianes, G., Kuang, W. J., Goeddel, D. V. & Ferrara, N. (1989) *Science* **246,** 1306–1309.
2. Ferrara, N. & Alitalo, K. (1999) *Nat. Med.* **5,** 1359–1364.
3. Rowe, D. H., Huang, J., Li, J., Manley, C., O'Toole, K. M., Stolar, C. J., Yamashiro, D. J. & Kandel, J. J. (2000) *J. Pediatr. Surg.* **35,** 977–981.
4. Rowe, D. H., Huang, J., Kayton, M. L., Thompson, R., Troxel, A., O'Toole, K. M., Yamashiro, D., Stolar, C. J. & Kandel, J. J. (2000) *J. Pediatr. Surg.* **35,** 30–32.
5. Holash, J., Wiegand, S. J. & Yancopoulos, G. D. (1999) *Oncogene* **18,** 5356–5362.
6. Holash, J., Maisonpierre, P. C., Compton, D., Boland, P., Alexander, C. R., Zagzag, D., Yancopoulos, G. D. & Wiegand, S. J. (1999) *Science* **284,** 1994–1998.
7. Zagzag, D., Friedlander, D. R., Margolis, B., Grumet, M., Semenza, G. L., Zhong, H., Simons, J. W., Holash, J., Wiegand, S. J. & Yancopoulos, G. D. (2000) *Pediatr. Neurosurg.* **33,** 49–55.
8. Rubenstein, J. L., Kim, J., Ozawa, T., Zhang, M., Westphal, M., Deen, D. F. & Shuman, M. A. (2000) *Neoplasia* **2,** 306–314.
9. Kunkel, P., Ulbricht, U., Bohlen, P., Brockmann, M. A., Fillbrandt, R., Stavrou, D., Westphal, M. & Lamszus, K. (2001) *Cancer Res.* **61,** 6624–6628.
10. Kim, E., Moore, J., Huang, J., Soffer, S., Manley, C. A., O'Toole, K., Middlesworth, W., Stolar, C. J., Kandel, J. J. & Yamashiro, D. J. (2001) *J. Pediatr. Surg.* **36,** 287–290.
11. Presta, L. G., Chen, H., O'Connor, S. J., Chisholm, V., Meng, Y. G., Krummen, L., Winkler, M. & Ferrara, N. (1997) *Cancer Res.* **57,** 4593–2599.
12. Holash, J., Davis, S., Papadopoulos, N., Croll, S. D., Ho, L., Russell, M., Boland, P., Leidich, R., Hylton, D., Burova, E., *et al.* (2002) *Proc. Natl. Acad. Sci. USA* **99,** 11393–11398.
13. Ruckman, J., Green, L. S., Beeson, J., Waugh, S., Gillette, W. L., Henninger, D. D., Claesson-Welsh, L. & Janjic, N. (1998) *J. Biol. Chem.* **273,** 20556–20567.
14. Tucker, C. E., Chen, L., Judkins, M. B., Farmer, J. A., Gill, S. C. & Drolet, D. W. (1999) *J. Chromatogr. Biomed. Appl.* **732,** 203–212.
15. Morikawa, S., Baluk, P., Kaidoh, T., Haskell, A., Jain, R. K. & McDonald, D. M. (2002) *Am. J. Pathol.* **160,** 985–1000.